A nanowire magnetic memory cell based on a periodic magnetic superlattice

J-F Song[1,2], J P Bird[3] and Y Ochiai[4]

[1] College of Electronic Science and Engineering, State Key Laboratory on Integrated Optoelectronics, Jilin University, Changchun 130023, People's Republic of China
[2] Institute of Semiconductors of Chinese Academy of Sciences, 100083, People's Republic of China
[3] Department of Electrical Engineering, University at Buffalo, The State University of New York, Buffalo, NY 14260-1920, USA
[4] Department of Electronics and Mechanical Engineering, Chiba University, 1-33 Yayoi, Inage-ku, Chiba 236-8522, Japan

Abstract
We analyse the operation of a semiconductor nanowire-based memory cell. Large changes in the nanowire conductance result when the magnetization of a periodic array of nanoscale magnetic gates, which comprise the other key component of the memory cell, is switched between distinct configurations by an external magnetic field. The resulting conductance change provides the basis for a robust memory effect, which can be implemented in a semiconductor structure compatible with conventional semiconductor integrated circuits.

The integration of nanoscale magnetic elements with semiconductor nanostructures, such as quantum wires and dots, offers the potential to realize a new class of electronics, characterized by reduced energy dissipation, increased switching speed and higher storage density, compared to conventional CMOS structures [1]. While there has been enormous progress in recent years in the development of metal-based magnetoelectronics, including devices that utilize the giant- and tunnelling-magnetoresistance effects, the development of analogous semiconductor structures is lagging far behind. (A notable exception is provided by hybrid Hall devices, in which small magnetic fields are sensed by modulating the fringing fields emanating from a nanomagnet on the top surface of a semiconductor junction [2, 3].)

Another area in which nanomagnetoelectronic devices have the potential to have an impact is that of memory architectures that utilize the distinct magnetization states of nanomagnets as the basis of a memory scheme. There is much interest, in particular, in exploiting the phenomenon of tunnelling magnetoresistance, observed in metallic magnetic multilayers, as the basis of realizing compact magnetic random-access memory (MRAM) [1]. In this paper, however, we consider a nanowire-based implementation of a magnetic memory cell, which
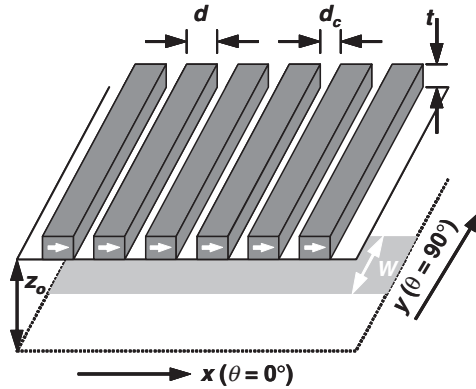
**Figure 1.** Schematic illustration of the memory structure.

exploits the unique features of quasi-one-dimensional electron transport in semiconductor nanowires to realize a significant memory effect.

The device that we study is shown in figure 1, and consists of a quantum wire of width W that is realized in a typical heterojunction, at a distance z_0 below its top surface. (For the purpose of implementation, we will assume here the case of a GaAs/AlGaAs heterojunction, for which the electron effective mass $m^* = 0.067\,m_0$.) A periodic array of equally spaced magnetic gates is formed on top of the heterojunction surface and the terminology that we use to denote the critical dimensions of these gates (t, d and d_c) is also indicated in the figure. In practice, such a device could be realized by conventional semiconductor microfabrication techniques, or by using self-assembled structures such as carbon nanotubes. In the coordinate system indicated in figure 1, the magnetic gates are taken to be aligned along the y-direction and each generates a normal magnetic field component in the plane of the nanowire, whose magnitude varies strongly along the x-direction. The precise form of this spatially varying magnetic field depends on the specific orientation of the gate magnetization [4], and in our discussion we properly account for overlap of the field distributions emanating from the different gates. We consider the situation where the magnetization of each gate is aligned either parallel, or antiparallel, to the $+x$-direction. This configuration is chosen largely for ease of implementation, since an analytical expression is available in this case for the resulting normal magnetic field distribution ($B_z(x)$; see equation (1) below) [4], and should only be stable with a strong magnetic field applied along the x-direction. An actual implementation might therefore involve a different gate geometry, for example making use of long nanomagnets whose ends are positioned in close proximity to the edges of the nanowire so that their fringing fields penetrate well into its interior (similar to the geometry considered in [2, 3]).

In a previous study [5], we analysed the influence of a structure related to that shown in figure 1 on the conductance of a *two-dimensional* electron gas (as opposed to a laterally confined nanowire), and the initial derivation here parallels much of the discussion provided in this earlier work. For a *single* gate, centred at $x = 0$, whose magnetization points along the $+x$-direction, the variation of the normal magnetic field component, as a function of the position in the 2DEG plane, is given by [4]

$$B_z(x) = B_0\left[K\left(x + \frac{d}{2}\right) - K\left(x - \frac{d}{2}\right) \right], \qquad B_0 = \frac{M_0 t}{d}, \qquad K(x) = \frac{z_0 d}{(x^2 + z_0^2)}. \qquad (1)$$

A similar equation is obtained when the magnetization points along the $-x$-direction, although its sign is now *opposite* at all points to that described by equation (1). The net magnetic
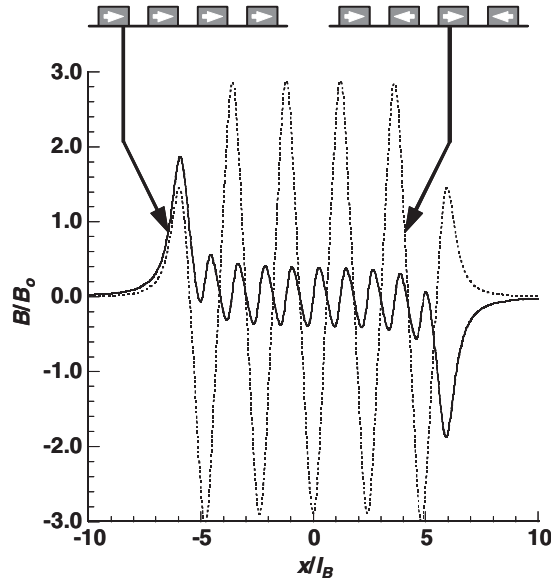
Figure 2. Normal magnetic field, $B_z(x)$, for the two different magnetization configurations. Solid line: parallel configuration. Dotted line: antiparallel configuration. The calculations are performed for an array comprised of ten magnetic gates.

field distribution resulting from an *array* of periodically spaced gates, such as that shown in figure 1, may then be determined by summing a series of terms of the form of equation (1). In the discussion that follows, we make use of the following parameters when discussing the effects of this magnetic field: the cyclotron frequency, $\omega_c \equiv eB_0/m^*$; the magnetic length, $l_B \equiv (\hbar/eB_0)^{0.5}$; and the cyclotron energy $E_0 \equiv \hbar\omega_c$. For a realistic comparison, we assume $B_0 = 0.1$ T in our calculations, yielding $E_0 = 0.17$ meV and $l_B = 81$ nm.

To solve for electron transmission in a spatially varying magnetic field, we make use of the time-independent Schrödinger equation and introduce this field via its associated vector potential (the vector potential corresponding to the magnetic field of equation (1) is given, for example, in [6]). Our analysis also includes a term due to the confining potential of the nanowire, $V(x, y)$. In the results presented here, we have taken $V(x, y) = 0$ at all points inside the wire and $V(x, y) = \infty$ everywhere else. We have also performed our calculations for a parabolic confining potential, however, and do not find any significant differences in our conclusions. Our analysis does *not* include a spin-related term, since we will generally be dealing with weak magnetic fields, for which spin degeneracy should not be lifted. Starting from the resulting Hamiltonian, we solve the Schrödinger equation numerically, making use of the results of scattering-matrix theory [7]. The solutions to this problem yield the energy-dependent transmission coefficients for the different subbands of the wire. By summing over all occupied subbands (at zero temperature), the total transmission coefficient, T, of the wire is obtained, after which the conductance can be determined by application of the Landauer formula, $G = (2e^2/h)T$. Simply for the purpose of demonstration, we assume here that $d = l_B$, $d_c = 0.2l_B$, $W = 2.5l_B$ and $z_0 = 0.5l_B$.

In figure 2, we show the calculated normal magnetic field profiles, $B_z(x)$, for the two distinct magnetization configurations of an array comprised of ten magnetic gates. (In the discussion that follows, we refer to the situation where the magnetization of each gate points in the same direction as the *parallel* case, and the one in which successive gates have oppositely
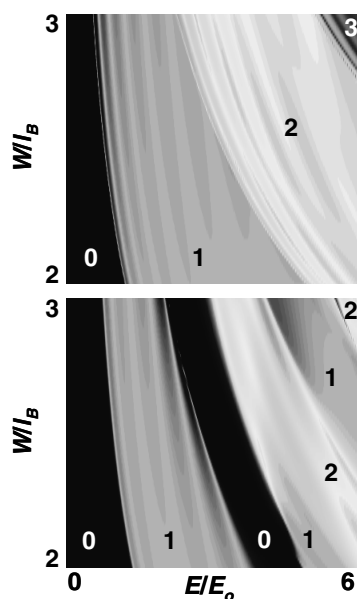
Figure 3. The greyscale shows the variation of the nanowire conductance with the Fermi energy
and wire width. The conductance in units of $2e^2/h$ is indicated by the indices in the different
regions of the figures. Upper panel: conductance for the parallel configuration. Lower panel:
conductance for the antiparallel configuration.

directed magnetizations as the *antiparallel* case.) It is clear from this figure that, by switching
between the parallel and antiparallel configurations, a significant change in the magnitude of
the magnetic field seen by electrons can be achieved. This change, in turn, results in large
modulations of the nanowire conductance, which should serve as the basis for a pronounced
memory effect. This characteristic is demonstrated in figure 3, where we show the variation of
the nanowire conductance on a greyscale, as a function of the wire width and electron Fermi
energy, for the two different magnetization configurations. The upper panel is obtained for the
parallel field case, for which the variation of $B_z(x)$ is relatively small (figure 2), and shows a
simple step-like increase of the conductance (the conductance in units of $2e^2/h$ is indicated
by the indices for the different regions of the figure) with increasing E and W. The vector
summation of the nanomagnet fringing fields in the antiparallel configuration results in a more
pronounced modulation of $B_z(x)$, and gives rise to very different conductance characteristics,
as is clear from the lower panel of figure 3. Of particular importance is the appearance of a
broad region of zero conductance, in the range of parameter space where the conductance in
the parallel configuration corresponds to $\sim$1–2 $\times$ $2e^2/h$. The appearance of such regions of
zero conductance is a well-known signature of the formation of a miniband structure, arising
from the presence of a periodic potential variation [8, 9]. In the present case, however, the
appearance of this gap at the Fermi level is a consequence of the periodicity of the magnetic
field generated by the magnetic gates.

The behaviour shown in figure 3 suggests the possibility of realizing a memory cell in
which changes in the magnetization of the magnetic gates result in a large modulation of the
conductance of the semiconductor nanowire. To further illustrate this point, in figure 4 we
plot the *difference* of the conductances (ΔG) obtained in the two magnetization configurations
as a function of the Fermi energy. In the energy range $\sim$3–4 $\times$ E/E_0, ΔG is comparable to
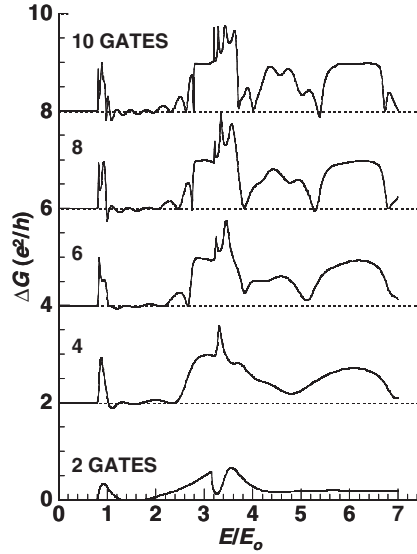
Figure 4. Difference in nanowire conductance for the two magnetization configurations, as a function of energy and the number of magnetic gates (indicated). Successive curves are shifted upwards by $2 \times 2e^2/h$.

the ON-state conductance itself ($\sim 2e^2/h$), so a very large memory effect can be expected. In figure 4, we also indicate the dependence of the memory effect on the number of magnetic gates in the structure. It is clear that a significant memory effect can be obtained when even just a small number of gates (2–4) are present—a significant result, since compactness is an important requirement in the design of a successful memory cell.

Having demonstrated the basic feasibility of the memory cell, we now give further consideration to the issues associated with its practical implementation. Switching between the distinct (parallel and antiparallel) magnetization configurations could be achieved by a few different approaches. The simplest of these would be to use an external magnetic field, applied along the easy axis of the nanomagnetic gates. To obtain a well-defined memory effect, one could use a structure with two pairs of gates, formed either with different geometries or from materials with distinct magnetic coercivities, which would then undergo magnetization reversal at different magnetic fields. For MRAM-related applications, the interest would be in generating the switching using a current flow through a write line, although in this case it seems unlikely that the nanowire-based cell could be made smaller than present MRAM cells. Nonetheless, the value of the approach proposed here is that the memory cell could be integrated onto the same semiconductor chip on which logic operations are performed. Another advantage of the nanowire-based approach is the very large modulation (close to 100%) of the readout current that can be expected when the memory cell is configured such that the current flow in the nanowire is associated with only the lowest subband (see figure 4). This is the regime where the Fermi energy $E_F \approx E_0$, and can be accessed by controlling the electron density in the nanowire, most easily by use of a back-gate voltage. While we have made specific assumptions in our analysis, regarding the form of the fringing fields generated by the magnetic gates, the basic memory operation should not be limited to the particular gate geometry that we consider. Rather, the important requirement is that it should be possible to switch between magnetization configurations that generate very different fringing field distributions in the nanowire. This

could be achieved, for example, by making use of long nanomagnets whose ends are positioned in close proximity to the edges of the nanowire, so that their fringing fields penetrate well into its interior. The direction of these field lines could then be reversed by using a weak magnetic field to switch the magnetization direction relative to the easy (long) axis. Although the exact conductance modulations would be different, in this case, to those shown in figures 3 and 4, the existence of distinct magnetization configurations should allow nonetheless for qualitatively similar behaviour, with significant regions of memory action (where $\Delta G \neq 0$).

In addition to the spatially varying magnetic field distribution, the memory effect is also a consequence of the quantized nature of transport in the nanowire. Consequently, this effect is expected to wash out at temperatures for which the thermal energy exceeds the one-dimensional subband separation in the wire. For high temperature operation, it will therefore be desirable to implement the memory cell in systems such as trench-grown InGaAs nanowires [10], which can have subband separations approaching 60 meV, or self-assembled structures, such as carbon nanotubes and rare-earth silicide nanowires [11]. In some of these systems, however, it may be important to also consider spin effects, which we have ignored thus far and which depend on the total magnetic field component (as opposed to the normal field). Neglecting spin should not be critical for the GaAs-based implementation that we have considered, however, for which the Zeeman splitting ($\sim$3 μeV) is much less than E_0 (170 μeV) for the value of B_0 (0.1 T) that we have assumed.

In conclusion, we have analysed the operation of a semiconductor nanowire-based memory cell. Large changes in the nanowire conductance result when the magnetization of a periodic array of nanoscale magnetic gates, which comprise the other key component of the memory cell, is switched between distinct configurations by an external magnetic field. The resulting conductance change provides the basis for a robust memory effect, which can be implemented in a semiconductor structure compatible with conventional semiconductor integrated circuits.

Acknowledgments

References

[1] Wolf S A, Awschalom D D, Buhrman R A, Daughton J M, von Molnar S, Roukes M L, Chtchelkanova A Y and Treger D M 2001 *Science* **294** 1488
[2] Johnson M, Bennett B R, Yang M J, Miller M M and Shanabrook B V 1997 *Appl. Phys. Lett.* **71** 974
[3] Monzon F G, Johnson M and Roukes M L 1997 *Appl. Phys. Lett.* **71** 3087
[4] Matulis A, Peeters F M and Vasilopoulos P 1994 *Phys. Rev. Lett.* **72** 1518
[5] Song J-F, Bird J P and Ochiai Y 2005 *Appl. Phys. Lett.* **86** 062106
[6] Lu M-W, Zhang L-D and Yan X-H 2003 *Nanotechnology* **14** 609
[7] Ferry D K and Goodnick S M 1997 *Transport in Nanostructures* (Cambridge: Cambridge University Press) chapter 3
[8] Leng M and Lent C S 1994 *Phys. Rev.* B **50** 10823
[9] Akis R and Ferry D K 1999 *Phys. Rev.* B **59** 7529
[10] Sugaya T, Bird J P, Ogura M, Sugiyama Y, Ferry D K and Jang K-Y 2002 *Appl. Phys. Lett.* **80** 434
[11] Lin J-F, Bird J P, He Z, Bennett P A and Smith D J 2004 *Appl. Phys. Lett.* **85** 281